



31 **Abstract:**

32 Lysine malonylation is a post-translational modification where a malonyl group, characterized by  
33 a negatively charged carboxylate, is covalently attached to the  $\epsilon$ -amino side chain of lysine,  
34 influencing protein structure and function. Our laboratory identified Mak upregulation in cartilage  
35 under aging and obesity, contributing to osteoarthritis (OA). Current antibody-based detection  
36 methods face limitations in identifying Mak targets. Here, we introduce an alkyne-functionalized  
37 probe, MA-diyne, which metabolically incorporates into proteins, enabling copper(I) ion-  
38 catalyzed click reactions to conjugate labeled proteins with azide-based fluorescent dyes or affinity  
39 purification tags. In-gel fluorescence confirms MA-diyne incorporation into proteins across  
40 various cell types and species, including mouse chondrocytes, adipocytes, Hek293T cells, and *C.*  
41 *elegans*. Pull-down experiments identified known Mak proteins such as GAPDH and Aldolase.  
42 The extent of MA-diyne modification was higher in Sirtuin 5-deficient cells suggesting these  
43 modified proteins are Sirtuin 5 substrates. Pulse-chase experiments confirmed the dynamic nature  
44 of protein malonylation. Quantitative proteomics identified 1136 proteins corresponding to 8903  
45 peptides with 429 proteins showing 1-fold increase in labeled group. Sirtuin 5 regulated 374 of  
46 these proteins. Pull down of newly identified proteins such as  $\beta$ -actin and Stat3 was also done.  
47 This study highlights MA-diyne as a powerful chemical tool to investigate the molecular targets  
48 and functions of lysine malonylation in OA conditions.

49

50 **Keywords:** alkyne-based probe, chondrocyte, click chemistry, lysine malonylation.

51

52

53

54

55

56

57

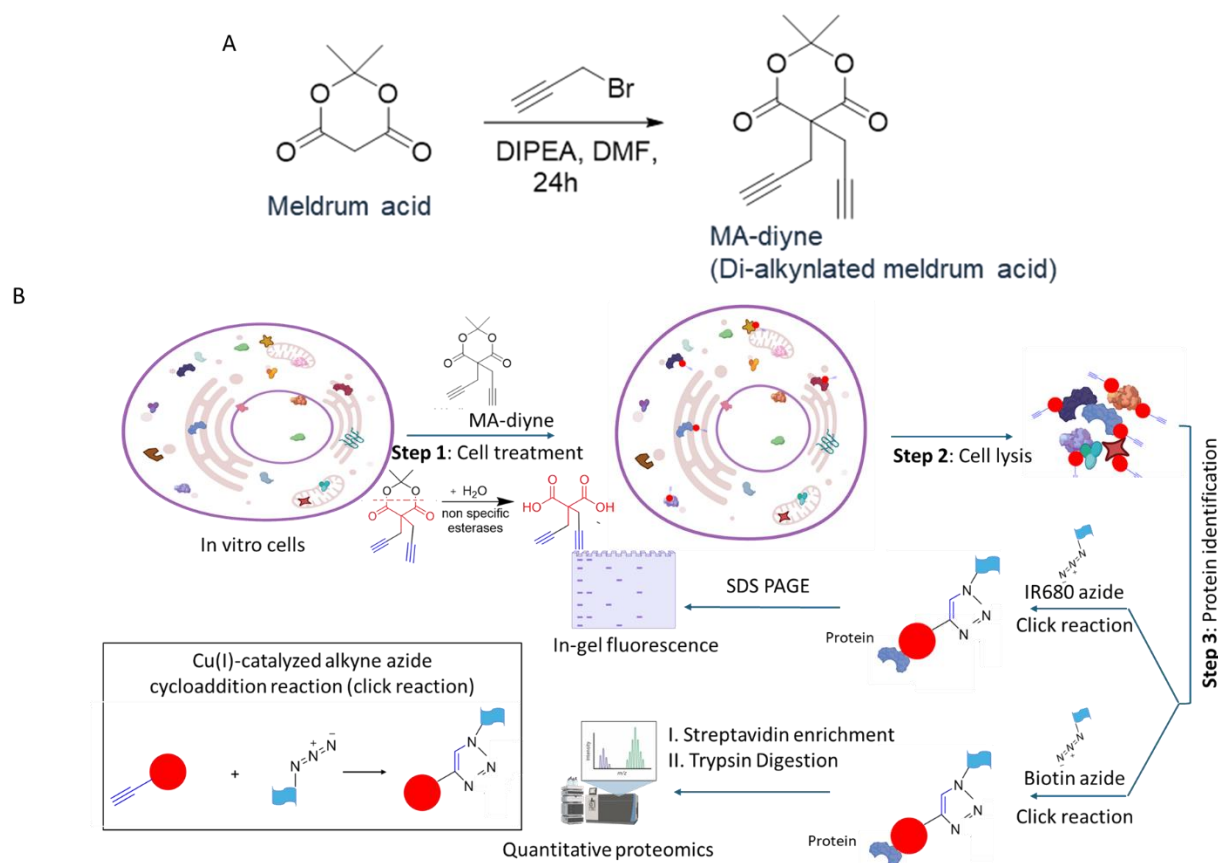
58

59

## 60 1. Introduction:

61 Post-translational modification of proteins refers to the biochemical covalent, enzymatic, and non-  
62 enzymatic addition of functional groups on proteins following their synthesis from ribosomes<sup>1</sup>.  
63 These functional groups can be small electrophilic biochemical metabolites like phosphate, sugars,  
64 nucleotides, methyl group, and acetyl group, long chain/short chain acyl chains like palmitoyl,  
65 malonyl groups, radicals generated from redox reactions like *S*-nitrosylation (SNO) and *S*-  
66 glutathionylation etc<sup>2</sup>. Post-translational modifications induce changes in amino acid chemical  
67 properties such as deamination, deamidation, citrullination, and oxidation, as well as protein  
68 autocatalysis that results in protein backbone cleavage. It offers complex and diverse functional  
69 roles to the existing proteome by regulating protein activity, structure and conformation, its  
70 location, and molecular interactions<sup>3</sup>. Post-translational covalent modification of proteins is  
71 fundamental to numerous cellular and biological functions. It plays a significant role in regulating  
72 normal cell physiology as well as the pathogenesis of diseases<sup>4</sup>. Lysine malonylation (Mak) is a  
73 reversible protein post-translational modification wherein a malonyl group is added to the  $\epsilon$ -amino  
74 group of the lysine residue in a protein. The addition of a negatively charged carboxylate group to  
75 the protein imparts significant changes in the protein's structure and function<sup>5</sup>. The reversible  
76 protein malonylation is theoretically regulated by acyltransferases and deacylases. The enzymes  
77 responsible for catalyzing the transfer of a malonyl group remain largely unidentified. However,  
78 recent work by Zang et al. has provided evidence that KAT2A is involved in histone malonylation<sup>6</sup>.  
79 Meanwhile, Sirtuin 5 (Sirt5), a class III lysine deacetylases member, is known for its lysine  
80 demalonylation activity along with its lysine desuccinylation function<sup>7,8</sup>. Our lab has previously  
81 demonstrated that deficiency of Sirt5 in mouse primary chondrocytes increases the global protein  
82 MaK level and disrupts cellular metabolism<sup>8</sup>. Identification of the protein substrates of Sirt5 is  
83 crucial for further elucidating the function of malonylation on the cellular metabolism and pinpoint  
84 the downstream targets. The anti-malonyl lysine antibody has been used previously to enrich and  
85 identify several malonylated proteins<sup>8-10</sup>. Antibody-based enrichment is generally based on the  
86 development of different antibody domains specific to targeting antigens with specific PTM,  
87 followed by immunoaffinity pull-down of target peptides from the protein lysates. However, this  
88 strategy suffers from a lack of specificity by missing some of the target PTM site due to the  
89 presence of adjacent PTM present on the same sequence<sup>11</sup>. To overcome this challenge, we took a  
90 chemical approach, utilizing an alkyne functionalized chemical probe to efficiently detect and

91 quantify protein substrates of lysine malonylation through fluorescence visualization and further  
92 identify them using a quantitative proteomics approach (Figure 1B). Alkyne functionalized probe  
93 allows metabolic detection of protein substrates by utilizing the copper(I) ion-catalyzed alkyne  
94 azide cycloaddition click chemistry to conjugate the labeled proteins with azide-fluorescent dyes  
95 or affinity purification tags<sup>12</sup>. This approach has been widely utilized in identifying several other  
96 types of PTMs including lipidation like myristoylation<sup>13,14</sup>, succinylation<sup>15,16</sup>, as well as  
97 acetylation<sup>17,18</sup> and glycosylation<sup>19,20</sup>. Previously, Bao et al. developed a malonic acid-based  
98 chemical probe called MalAM-yne to detect lysine malonylation<sup>21</sup>. In this study, we designed and  
99 synthesized a novel Meldrum's acid-based probe, i.e. MA-diyne, as a better synthetic alternative  
100 to the previously reported probe<sup>21</sup>. Meldrum's acid or isopropylidene malonate is a condensation  
101 product of malonic acid and acetone. We developed this new probe by functionalizing Meldrum  
102 acid or isopropylidene malonate with alkylation under control conditions (Figure 1A). We  
103 hypothesize that Meldrum acid will be readily absorbed into the cells due to its cyclic structure  
104 and subsequently will get linearized to form a malonyl group by an unknown action of intracellular  
105 esterases, thus leading to effective detection and identification of the malonylated proteins.



106 **Figure 1:** A. Design, synthesis, and characterization of MA-diyne. B. Schematic description of the  
107 workflow to detect and identify lysine malonylated proteins using MA-diyne.

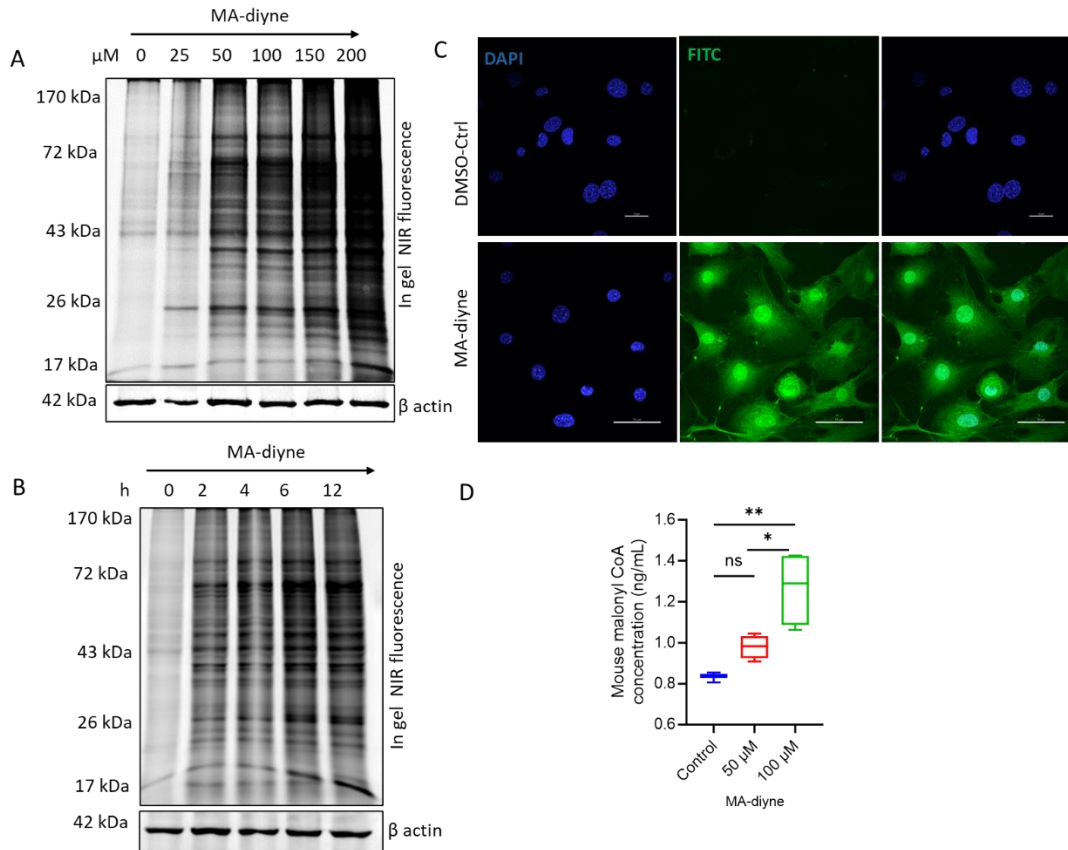
## 108 **2. Results and discussion:**

109 2.1. Chemical synthesis: Bao et al 2013 were the first to report a chemical probe with an alkyne  
110 handle on the malonate group named Mal-yne<sup>21</sup>. However, they modified this probe to increase  
111 cell permeability by masking the carboxylate sides with two acetoxymethyl groups and called it  
112 MalAM-yne. In this report, we selected an alternative approach by adding an alkyne handle to  
113 Meldrum acid or isopropylidene malonate. The high reactivity of this molecule is attributed to the  
114 methylene group present between the carbonyl group and this site was utilized to add the propargyl  
115 unit to meldrum acid under controlled conditions. Thereby, we generated dipropargyl meldrum  
116 acid or MA-diyne through the following chemical synthesis (Figure 1A). The proposed probe has  
117 a better ability of hydrolysis in the presence of esterase than the probe MalAM-yne by Bao et al  
118 2013<sup>21</sup>. The synthesis involves di-alkynylation on commercially available Meldrum acid. The  
119 reaction is performed under mild conditions such as DIPEA (diisopropyl ethylamine) with  
120 anhydrous DMF solvent under room temperature. The reaction is stirred for 24 hr. After the  
121 working up of the reaction, the product is taken for purification. The initial purification of the MA-  
122 diyne product is carried out with normal SiO<sub>2</sub> which leads to ring-opening of MA-diyne due to its  
123 acidity. Later, SiO<sub>2</sub> was neutralized with triethylamine and then purification was carried out. The  
124 pure product is characterized by <sup>1</sup>H NMR spectroscopy [<sup>1</sup>H NMR (400 MHz): δ 1.84 (s, 6H), 2.18,  
125 (t, *J* = 5.2 Hz, 2H), 2.88 (d, *J* = 2.8 Hz, 4H) ppm. The respective assignments and full spectra of  
126 MA-diyne are given as supplementary information (Scheme SF1 and SF2). The described method  
127 (one step) is simple, faster, and gives maximum yield (40%) compared to the previously reported  
128 three-step method (overall yield; 23%). The yield limitation to 40% in the present method arises  
129 from the ring-opening reaction of Meldrum's acid under the specified conditions.

130 **2.2 MA-diyne can be metabolically incorporated into cellular proteins.** Our first inquest was  
131 to analyze whether MA-diyne can metabolically incorporate into proteins similarly to malonyl-  
132 CoA. Therefore, we incubated mouse primary chondrocytes with different concentrations (0- 200  
133 μM) of MA-diyne in complete medium for 6 h (a working stock of 100 mM was prepared by  
134 dissolving MA-diyne in DMSO; DMSO was taken as control). The protein lysate was collected  
135 after harvesting the cells and was subjected to azide-alkyne click chemistry to conjugate the alkyne

136 side group with IR680 azide dye. The clicked proteins were then resolved on SDS-PAGE and  
137 scanned using in-gel IR fluorescence imager. The result showed that there was a dose-dependent  
138 increase of MA-diyne labeling of global proteins with the optimal concentration at less than 50  
139  $\mu$ M MA-diyne (Figure 2A). To analyze the time required for the metabolic labeling, a time-  
140 dependent experiment was conducted by incubating the primary chondrocytes with 100  $\mu$ M of  
141 MA-diyne at different time points ranging from 0-12 h. MA-diyne was able to efficiently label the  
142 proteins in no more than 2 h (Figure 2B). Interestingly, we observed that MA-diyne showed more  
143 bands in gel fluorescence compared to western blot analysis of the same proteins from primary  
144 chondrocytes using a commercial anti-KMal antibody (Supplementary Figure 1). The dose and  
145 time-dependent experiment demonstrated the efficient labeling of proteins by MA-diyne.

146 To confirm that the signal achieved in the primary chondrocytes after treatment with MA-diyne is  
147 due to metabolic labeling and not due to nonspecific binding, we used qualitative fluorescence  
148 imaging to visualize the labeled proteins. The primary chondrocytes were cultured on coverslips  
149 overnight and treated with different doses of MA-diyne for 6 h. The cells were immediately fixed  
150 using ice-cold 4% paraformaldehyde and then permeabilized. The cells were then subjected to  
151 click reaction using Carboxyrhodamine 110 Azide for 1 h. The cells on the coverslips were  
152 mounted on clean glass slides using mounting reagent with DAPI. Control samples were generated  
153 by performing the same procedure without MA-diyne or Carboxyrhodamine 110 Azide. The slides  
154 were imaged using Nikon A1R confocal microscopy under 60X magnification (Figure 2C and  
155 supplementary Figure 2). MA-diyne was found to be rapidly absorbed into the cells which was  
156 demonstrated by the intensity of labeling only in the samples treated with MA-diyne followed by  
157 click reaction with Carboxyrhodamine 110 Azide but not in the control samples incubated with  
158 Carboxyrhodamine 110 Azide only or samples treated with only MA-diyne (supplementary Figure  
159 2). We observed widespread protein labeling in various cell compartments, prompting us to  
160 conduct quantitative proteomics. However, to ensure the labeling is due to the malonyl-CoA  
161 formed by the acyclization of Meldrum acid, we estimated the concentration of malonyl-CoA  
162 formed in the cells after incubating the cells with MA-diyne in different concentrations and  
163 compared it with control cells without MA-diyne. We observed a significant increase in the  
164 concentration of malonyl CoA at 100  $\mu$ M. However, as protein labeling by MA-diyne increases  
165 with incubation time, malonyl-CoA concentration may also depend on the time needed for MA-  
166 diyne uptake and linearization.



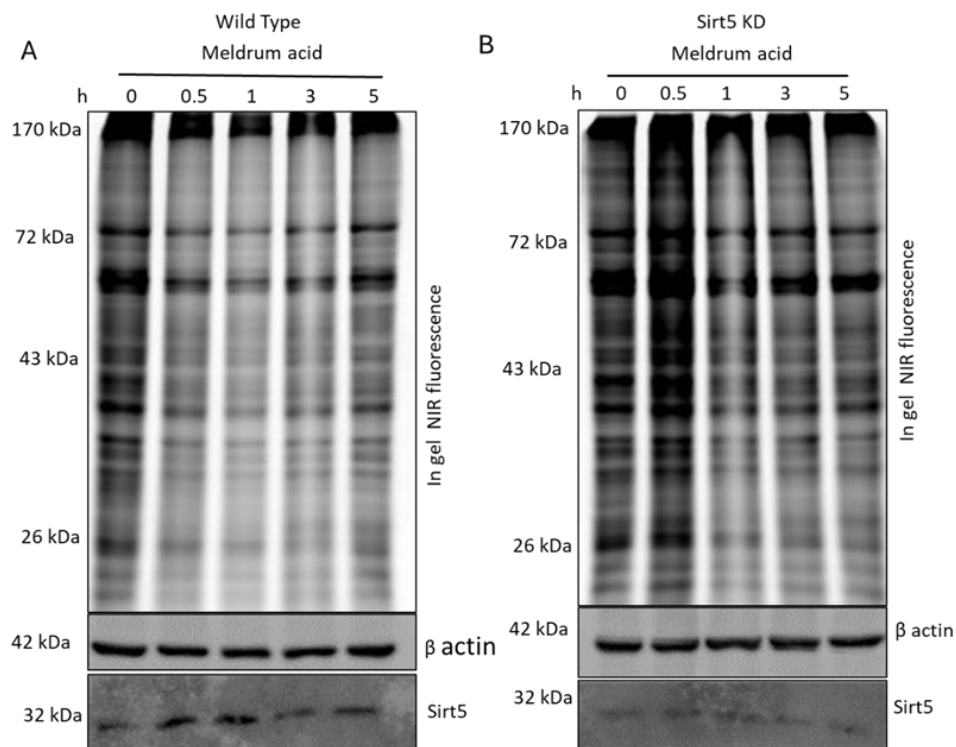
167

168 **Figure 2: Assessment of the ability of MA-diyne to metabolically label proteins.** A. Mouse  
169 primary chondrocytes were incubated with the indicated concentration of MA-diyne for 6 h. The  
170 cell lysates were then clicked with IR680-azide followed by in-gel fluorescence analysis. B. Mouse  
171 primary chondrocytes were incubated with 100  $\mu\text{M}$  of MA-diyne for the indicated time points.  
172 Cell lysates were then clicked with IR680- azide and in-gel fluorescence analyses.  $\beta$  actin was used  
173 as a loading control. C. Confocal microscopic fluorescence image depicting the ready uptake of  
174 the MA-diyne into the cells and subcellular localization of malonylated proteins in the primary  
175 chondrocytes. D. Box plot showing the concentration of intracellular malonyl-CoA in the cells  
176 after incubation with different concentrations of MA-diyne for 4 h.  $n=4$ . Data are presented as  
177 mean  $\pm$  SEM. Three group comparisons were evaluated using two-way ANOVA. Significance is  
178 noted as ns  $p>0.05$ , \* $p<0.05$ , and \*\* $p<0.01$ .

179 **2.3 MA-diyne was dynamically removed from the proteins representing the reversible nature**  
180 **of lysine malonylation.** Lysine modifications like succinylation, glutarylation, and malonylation  
181 are reversible forms of protein post-translational modifications<sup>9,22,23</sup>. Although the enzyme



182 responsible for adding a malonyl group to the proteins is still unknown, Sirtuin 5 (Sirt5) has been  
183 well-documented as the enzyme responsible for removing this modification<sup>6,24</sup>. To examine  
184 whether the labeling by MA-diyne is also reversible, we conducted a pulse-chase experiment. The  
185 wild type and Sirt5 knockdown primary chondrocytes were first incubated with 200  $\mu$ M MA-diyne  
186 for 1 h. The cells were then washed and chased with 200  $\mu$ M Meldrum acid for 0-5 h. The cells  
187 were harvested at different time points, and protein lysates were conjugated with IR680-azide dye.  
188 The in-gel fluorescence imaging reveals that the labeling signal by MA-diyne in wild-type primary  
189 chondrocytes started fading after 0.5 h of Meldrum acid incubation, indicating the removal of MA-  
190 diyne labeling from the proteins (Figure 3A). In comparison, in Sirt5 knockdown cells, the labeling  
191 signal with MA-diyne became more intense after 0.5 h compared to the baseline level and there is  
192 less removal of MA-diyne from the labeled proteins compared to the wild-type cells (Figure 3B).  
193 We also noticed that the labeling by MA-diyne was not modulated by the endogenous levels of  
194 malonyl-CoA, evidenced by no difference between wild type and cells deficient of acetyl-CoA  
195 carboxylase (ACC1), an enzyme that produces malonyl-CoA (supplementary figure 3). These  
196 results suggested that the metabolically modified proteins by MA-diyne could be substrates of  
197 Sirt5 demalonylase and the process is reversible.





199 **Figure 3: Pulse-chase experiment to determine the dynamic nature of lysine malonylation.**

200 Wild-type mouse primary chondrocytes (A) and Sirt5KO primary chondrocytes (B) were labeled  
201 with 200  $\mu$ M MA-diyne for 1 h and then pulse chased with 200  $\mu$ M Meldrum acid (precursor).  
202 The lysates were collected at the indicated time points followed by a click reaction with IR680-  
203 azide and in gel fluorescence analysis.  $\beta$  actin was used as a loading control. The same blot was  
204 probed with an anti-Sirt5 antibody to quantify the knockdown efficiency.

205 **2.4 MA-diyne successfully identified putative malonylated proteins.** Our previous studies have  
206 demonstrated the important role of Sirt5 in chondrocyte metabolism by regulating the  
207 malonylation of metabolic enzymes<sup>25-28</sup>. We have also used proteomics to identify the malonylome  
208 in chondrocytes using the traditional Kmal PTMscan antibody-based enrichment method<sup>28</sup>. We  
209 reported the enrichment of 1000 peptides corresponding to 469 proteins. Herein this report, we  
210 applied a chemoproteomics-based approach to enrich malonylated proteins from primary  
211 chondrocytes using MA-diyne. Wild type and Sirt5 knockdown primary chondrocytes were  
212 labeled with MA-diyne (100  $\mu$ M) for 6 h and then the protein lysates were conjugated to biotin  
213 azide through azide-alkyne copper cycloaddition reaction. The biotin-conjugated proteins were  
214 then immuno-precipitated using avidin agarose beads. The beads were thoroughly washed with  
215 HPLC water to prevent detergent or protease inhibitor contamination in the LCMS, followed by  
216 addition of 9M urea wash. The beads were then subjected to reductive alkylation with dithiothreitol  
217 (DTT) and iodoacetamide (IAA), on bead trypsin digestion, and desalting. The enriched peptides  
218 were then subjected to bottom-up quantitative proteomics on Orbitrap Astral Instrument. A total  
219 of 1136 proteins corresponding to 8903 peptides across all samples (supplementary data excel 1)  
220 were identified, which was 2.4 times more than the proteins we identified before using Kmal  
221 PTMscan antibody enrichment<sup>28</sup>. 430 proteins were seen to show a more than 1-fold increase in  
222 probe group in comparison to the control group with more than 6 unique peptides (supplementary  
223 data excel 2). This indicated that MA-diyne could enrich malonylated proteins. The enrichment of  
224 proteins in the control group accounts for the endogenously biotinylated proteins which might have  
225 been enriched with avidin beads. Furthermore, 387 out of the 430 proteins were found to have  
226 more than 1-fold increase in the Sirt5 knockdown + MA-diyne group in comparison to the wild  
227 type + MA-diyne group (supplementary data excel 2). This indicates that Ma-diyne successfully  
228 enriched proteins which are regulated by Sirt5 demalonylase enzyme. Since the peptides search  
229 was not done for the modified peptides (due to the difficulty in eluting the biotinylated peptides

230 after on-bead trypsinization), we compared the 8903 peptides to those modified sites identified by  
 231 Kmal PTMscan antibody enrichment in our previous study. Interestingly, some of the peptides  
 232 sequences identified in MA-diyne enrichment matched with the sequence identified in the LC-  
 233 MS/MS data acquired after enrichment with the Kmal PTMscan antibody<sup>28</sup> (Table 1). All these  
 234 observations indicate that MA-diyne can efficiently detect and identify lysine malonylated  
 235 proteins. Since our data lack site-specific identification of malonylation, our lab is currently  
 236 exploring alternative proteomic approaches to identify malonylated sites on proteins detected by  
 237 MA-diyne in MA-diyne treated primary chondrocytes. Further, these proteins will be pulled down  
 238 using enrichment tags and analyzed in LC-MS/MS for the signature satellite peaks.

239 **Table 1: List of manually validated peptides sequences with modified malonylated sites**

Protein description	Accession number	Peptide sequence identified with Kmal enrichment	Corresponding peptides enriched in MA-diyne treatment
L-lactate dehydrogenase A chain	<a href="#">P06151</a>	IVSSKDYCVTANSK*	IVSSKDYCVTANSK, DYCVTANSK
Glucose-6-phosphate isomerase	<a href="#">P06745</a>	ELQAAGK*SPEDLEK	ELQAAGKSPEDLEK
Annexin A1	<a href="#">P10107</a>	K*ALLALAK	KALLALAK
Annexin A2	<a href="#">P07356</a>	ASM#K*GLGTDEDSLIEIICSR ELYDAGVK*R TK*GVDEVTIVNILTNR	TPAQYDASELKASM#K, TPAQYDASELK, GLGTDEDSLIEIICSR ELYDAGVKR TKGVDEVTIVNILTNR
Calmodulin-1	<a href="#">P0DP26</a> ; <a href="#">P0DP27</a> ; <a href="#">P0DP28</a>	EAFSLFDK*DGDGTITTK	EAFSLFDK, DGDGTITTK
Protein S100-A4	<a href="#">P07091</a>	ELPSFLGK*R	ELPSFLGK

Actin, cytoplasmic 1	<a href="#">P60710</a> ; <a href="#">P63260</a>	K*DLYANTVLSGGTTM#YPGIADR	KDLYANTVLSGGTTM#YP GIADR
Src substrate cortactin	<a href="#">Q60598</a>	SAVGHEYQSK*LSK	SAVGHEYQSK
Moesin	<a href="#">P26041</a>	AK*FY PEDVSEELIQDITQR	AKFY PEDVSEELIQDITQR
Vinculin	<a href="#">Q64727</a>	NLGPGM#TKM#AK*	NLGPGMTK
Glyceraldeh yde-3- phosphate dehydrogen ase	<a href="#">P16858</a>	VIHDNFGIVEGLM#TTVHAITATQK* TVDGPSGK	VIHDNFGIVEGLM#TTVH AITATQK
Glyceraldeh yde-3- phosphate dehydrogen ase	<a href="#">P16858</a>	LVINGK*PITIFQERDPTNIK	LVINGKPITIFQERDPTNIK
Glyceraldeh yde-3- phosphate dehydrogen ase	<a href="#">P16858</a>	TVDGPSGK*LWR	TVDGPSGKLWR
Peptidyl- prolyl cis- trans isomerase A	<a href="#">P17742</a>	SIYGEK*FEDENFILK	SIYGEKFEDENFILK
Pyruvate kinase PKM	<a href="#">P52480</a>	CCSGAIIVLTK*SGR	CCSGAIIVLTK
Myosin regulatory light chain 12B	<a href="#">Q3THE2</a>	K*GNFN YIEFTR	GNFN YIEFTR

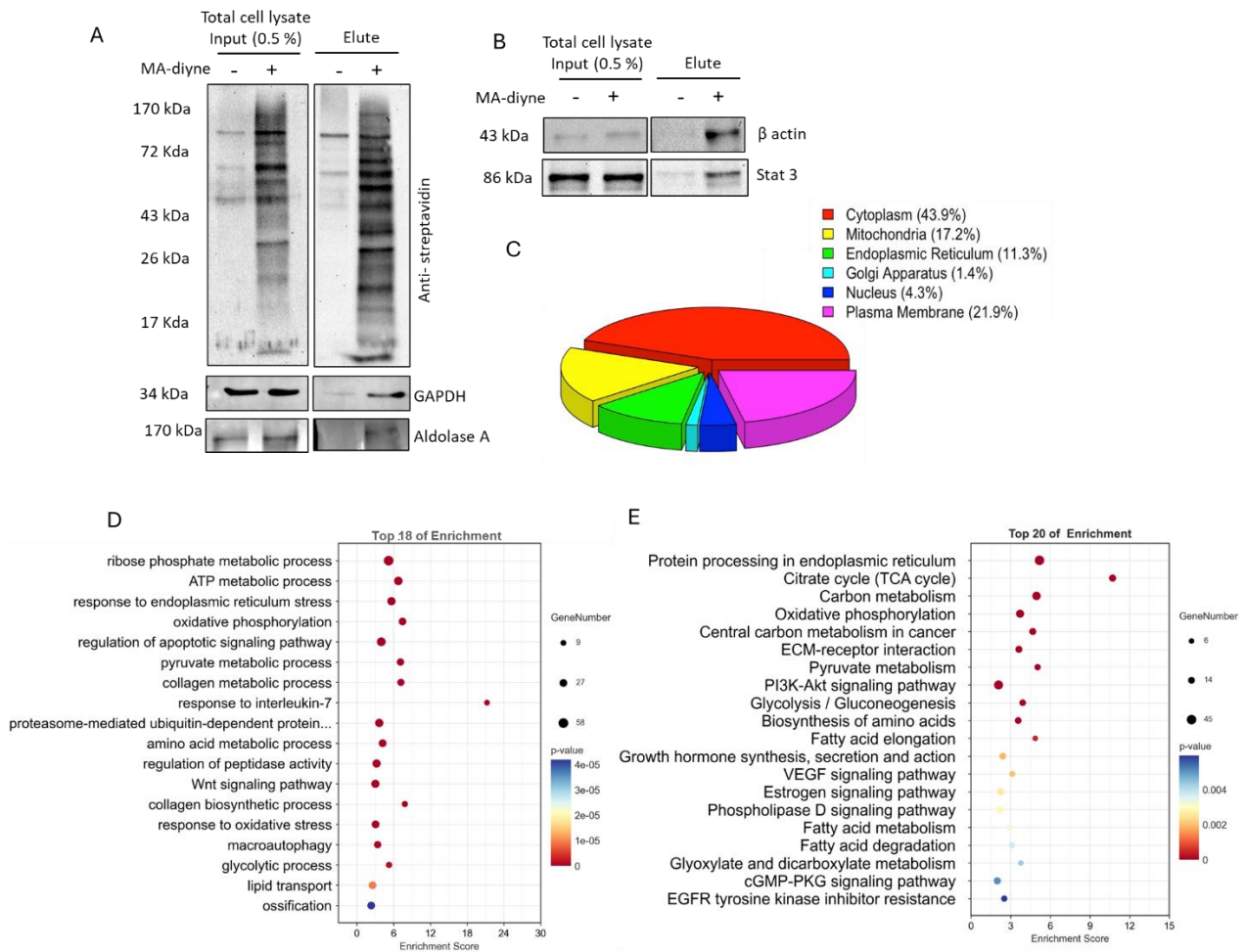
High mobility group protein B1	<a href="#">P63158</a>	K*HPDASVNFSEFSK	KHPDASVNFSEFSK
Elongation factor 1-alpha 1	<a href="#">P10126</a>	SGK*KLEDGPK	THINIVVIGHVDSGK, KLEDGPK
Elongation factor 2	<a href="#">P58252</a>	EDLYLK*PIQR	EDLYLKPIQR

240

241 We then conducted a pull-down experiment to validate further that MA-diyne could enrich  
242 malonylated proteins. The eluted protein from the avidin beads in a separate experiment were  
243 resolved on the SDS-PAGE followed by immunoblotting against antibodies for some already  
244 known malonylated proteins, ALDOA (Fructose-bisphosphate aldolase A)<sup>28</sup> and GAPDH  
245 (Glyceraldehyde-3- phosphate dehydrogenase)<sup>29</sup>. The detection of GAPDH and ALDOA by  
246 western blot analysis of the eluted proteins from the beads (Figure 4A) confirmed that MA-diyne  
247 can indeed enrich malonylated proteins. We could also pull down other novel proteins in our  
248 proteomics list like Stat3, and  $\beta$  actin that haven't been reported before (Figure 4B).

249 Gene ontology (GO) and pathway analysis of the identified proteins revealed that the malonylated  
250 proteins are localized differentially in various subcellular compartments including cytoplasm,  
251 plasma membranes, endoplasmic reticulum, nucleus, mitochondria, and Golgi apparatus of the  
252 primary chondrocytes (Figure 4C and supplementary excel 3). These findings align with similar  
253 subcellular localization patterns of malonylated proteins observed in other cell types, such as  
254 plants<sup>30</sup>, prokaryotes<sup>31</sup>, parasites<sup>32</sup> and mammalian cells<sup>9</sup>. GO analysis based on the biological  
255 processes revealed that the identified malonylated proteins belonged to processes related to  
256 musculoskeletal tissues like collagen biosynthesis, and ossification. Additionally, it was revealed  
257 that malonylated proteins are highly involved in glucose, amino acid, and pyruvate metabolic and  
258 lipid transport processes. The identified proteins are also enriched in biological processes like  
259 ribose phosphate metabolism, ATP production, TCA cycle, glycolysis, and oxidative  
260 phosphorylation (Figure 4D and supplementary excel 4). These findings are consistent with  
261 previous reports on the involvement of lysine malonylation in regulation of metabolic disorders

262 like type 2 diabetes<sup>33</sup>, cardiovascular diseases<sup>34</sup>, osteoarthritis<sup>25,35</sup> etc. We also observed the role  
 263 of malonylated proteins in the mechanisms related to the quality control of proteins such as  
 264 response to endoplasmic reticulum stress<sup>5</sup>, autophagy<sup>36</sup> and proteasome-mediated protein  
 265 processing (Figure 4D and supplementary excel 4). KEGG analysis of the identified malonylated  
 266 proteins revealed regulation of several signaling pathways like VEGF, Wnt signaling, cGMP-PKG,  
 267 PI3K-AKT, estrogen signaling, EGFR tyrosine kinase inhibitor resistance, growth hormone  
 268 synthesis and secretion, phospholipase D signaling pathways etc (Figure 4E and supplementary  
 269 excel 5).

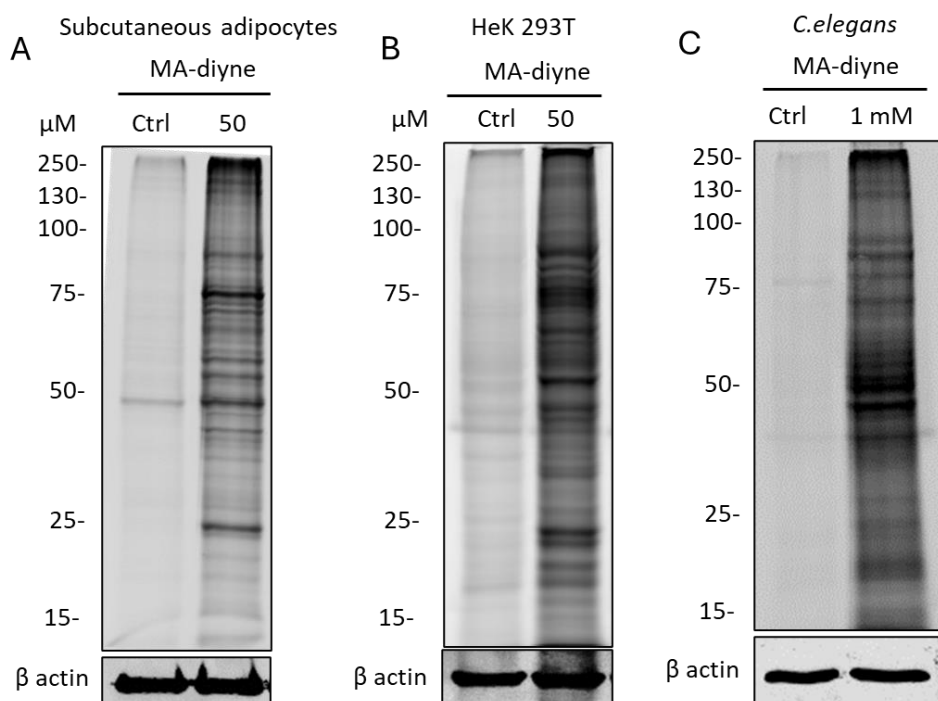


270

271 **Fig 4. Validation of Lysine malonylated protein targets of MA-diyne.** A. Pull down of known  
 272 malonylated proteins such as GAPDH and Aldolase A after enrichment using avidin beads. n=2.  
 273 B. pull down of newly identified proteins after MA-diyne enrichment. n=2. C. Pie chart depicting  
 274 the percentage of malonylated proteins found in different subcellular compartments by GO

275 analysis. D. distribution of enriched proteins based on their biological process by GO analysis, E.  
276 KEGG pathway analysis of the enriched proteins. p value < 0.05.

277 **2.5 MA-diyne can detect lysine malonylation in a wide range of cell types *in vitro*.** To assess  
278 the applicability of MA-diyne probe in detecting malonylated proteins in different types of cells,  
279 we analyzed the metabolic labeling profile of MA-diyne in subcutaneous primary adipocytes  
280 (Figure 5A), and Hek 293T cell lines (Figure 5B). Both cells exhibited robust MA-diyne signaling  
281 compared to the control suggesting successful metabolic incorporation of MA-diyne into cellular  
282 proteins. In addition, we assessed whether MA-diyne can be used to metabolically label proteins  
283 of *C.elegans*. We incubated live *C.elegans* with 1mM MA-diyne for 6 h with constant shaking and  
284 then lysed the worms to extract proteins. The proteins were then conjugated with IR680 azide. In-  
285 gel fluorescence analysis revealed that MA-diyne resulted in a robust labeling of malonylated  
286 proteins (Figure 5C). The route for the metabolic labeling is unclear but it is assumed that MA-  
287 diyne could have penetrated *C.elegans* cells either via the esophageal route or epidermal  
288 absorption/passive diffusion.



289

290 **Figure 5:** MA-diyne can detect lysine malonylated proteins in other cells like primary  
291 subcutaneous adipocytes, Hek293T cells and *C. elegans*, n=2



### 292 3. Conclusion

293 In summary, we have developed a novel chemical probe, MA-diyne for identifying and quantifying  
294 the protein malonylation in primary chondrocytes and several other types of cells. This probe was  
295 synthesized by adding a propargyl group to the mel drum acid for utilizing the conventional  
296 chemoproteomic approach to pull down the malonylated proteins. MA-diyne was observed to be  
297 readily uptaken into the cells and after getting acylized to malonyl-CoA by the action of  
298 intracellular esterases, it then metabolically labeled the proteins. It was also observed that labeling  
299 by MA-diyne was dynamic and regulated by the demalonylase enzyme, Sirt5. Moreover, the  
300 labeling by MA-diyne was observed to be nonenzymatic and not dependent on the endogenous  
301 levels of malonyl CoA. Quantitative proteomics could identify a significantly larger number of  
302 proteins than our previous attempt with the Kmal PTMscan antibody. Moreover, this further  
303 enables us to validate the enzymatic function of several identified metabolic proteins and their role  
304 in the progression of osteoarthritis.

### 305 Acknowledgements

306 We thank the following funding support: Hevolution Foundation AGE award AGE-008 (SZ, HL),  
307 National Institutes of Health grant R01AR081804 (SZ, HL), National Institutes of Health grant  
308 R15AR080813 (SZ, HL), Arthritis National Research Foundation, American Society for Bone and  
309 Mineral Research FIRST award (SZ), Rheumatology Research Foundation Innovative Award (SZ),  
310 Osteopathic Heritage Foundation Ralph S. Licklider, D.O. Endowed Professorship (SZ). We thank  
311 the staff (including Tammy Mace, Angela Smith, Shawn Rosensteel, and Scott Carpenter) at the  
312 animal facility in the Life Science Building for their excellent care for our animals. We thank Dr.  
313 Vishwajeet Puri, Dr. Craig Nunemaker, and Dr. Kevin Lee for providing the cell lines. We also  
314 thank Dr. Nathaniel Szewczyk for helping us conduct the labeling in *C.elegans*. We acknowledge  
315 the help from Proteomics Core Facility at the Cell Signaling Technology Company for their help  
316 with the proteomics assay.

317

318

319 **Reference:**

- 320 1 Lee, J. M., Hammarén, H. M., Savitski, M. M. & Baek, S. H. Control of protein stability by post-  
321 translational modifications. *Nature Communications* **14**, 201 (2023).  
322 <https://doi.org/10.1038/s41467-023-35795-8>
- 323 2 Zhong, Q., Xiao, X., Qiu, Y., Xu, Z., Chen, C., Chong, B., Zhao, X., Hai, S., Li, S., An, Z., & Dai,  
324 L. Protein posttranslational modifications in health and diseases: Functions, regulatory  
325 mechanisms, and therapeutic implications. *MedComm* (2020) **4**, e261 (2023).  
326 <https://doi.org/10.1002/mco2.261>
- 327 3 Dutta, H. & Jain, N. Post-translational modifications and their implications in cancer. *Front Oncol*  
328 **13**, 1240115 (2023). <https://doi.org/10.3389/fonc.2023.1240115>
- 329 4 Pan, S. & Chen, R. Pathological implication of protein post-translational modifications in cancer.  
330 *Mol Aspects Med* **86**, 101097 (2022). <https://doi.org/10.1016/j.mam.2022.101097>
- 331 5 Zou, L., Yang, Y., Wang, Z., Fu, X., He, X., Song, J., Li, T., Ma, H., & Yu, T. Lysine Malonylation  
332 and Its Links to Metabolism and Diseases. *Aging Dis* **14**, 84-98 (2023).  
333 <https://doi.org/10.14336/ad.2022.0711>
- 334 6 Zhang, R., Bons, J., Scheidemantle, G., Liu, X., Bielska, O., Carrico, C., Rose, J., Heckenbach, I.,  
335 Scheibye-Knudsen, M., Schilling, B., & Verdin, E. Histone malonylation is regulated by SIRT5 and  
336 KAT2A. *iScience* **26**, 106193 (2023). <https://doi.org/10.1016/j.isci.2023.106193>
- 337 7 Rardin, M. J., He, W., Nishida, Y., Newman, J. C., Carrico, C., Danielson, S. R., Guo, A., Gut, P.,  
338 Sahu, A. K., Li, B., Uppala, R., Fitch, M., Riiff, T., Zhu, L., Zhou, J., Mulhern, D., Stevens, R. D.,  
339 Ilkayeva, O. R., Newgard, C. B., Jacobson, M. P., ... Verdin, E.. SIRT5 regulates the mitochondrial  
340 lysine succinylome and metabolic networks. *Cell Metab* **18**, 920-933 (2013).  
341 <https://doi.org/10.1016/j.cmet.2013.11.013>
- 342 8 Nishida, Y., Rardin, M. J., Carrico, C., He, W., Sahu, A. K., Gut, P., Najjar, R., Fitch, M.,  
343 Hellerstein, M., Gibson, B. W., & Verdin, E. SIRT5 Regulates both Cytosolic and Mitochondrial  
344 Protein Malonylation with Glycolysis as a Major Target. *Molecular cell* **59** 2, 321-332 (2015).
- 345 9 Peng, C. , Lu, Z., Xie, Z., Cheng, Z., Chen, Y., Tan, M., Luo, H., Zhang, Y., He, W., Yang, K.,  
346 Zwaans, B. M., Tishkoff, D., Ho, L., Lombard, D., He, T. C., Dai, J., Verdin, E., Ye, Y., & Zhao, Y.  
347 The first identification of lysine malonylation substrates and its regulatory enzyme. *Mol Cell*  
348 *Proteomics* **10**, M111.012658 (2011). <https://doi.org/10.1074/mcp.M111.012658>
- 349 10 Du, J., Zhou, Y., Su, X., Yu, J.J., Khan, S., Jiang, H., Kim, J., Woo, J., Kim, J.H., Choi, B.H., He,  
350 B. Chen., W, Zhang., S, Cerioe, R.A., Auwerx, J., Hao Q., Lin H. Sirt5 is a NAD-dependent protein  
351 lysine demalonylase and desuccinylase. *Science* **334**, 806-809 (2011).  
352 <https://doi.org/10.1126/science.1207861>

- 353 11 Bock, I., Dhayalan A, Kudithipudi S, Brandt O, Rathert P, Jeltsch A. Detailed specificity analysis  
354 of antibodies binding to modified histone tails with peptide arrays. *Epigenetics* **6**, 256-263 (2011).  
355 <https://doi.org/10.4161/epi.6.2.13837>
- 356 12 Sletten, E. M. & Bertozzi, C. R. Bioorthogonal chemistry: fishing for selectivity in a sea of  
357 functionality. *Angew Chem Int Ed Engl* **48**, 6974-6998 (2009).  
358 <https://doi.org/10.1002/anie.200900942>
- 359 13 Gong, X., Feng, Y. & Tang, H. A metabolic labeling protocol to enrich myristoylated proteins from  
360 *Caenorhabditis elegans*. *STAR Protoc* **2**, 101013 (2021).  
361 <https://doi.org/10.1016/j.xpro.2021.101013>
- 362 14 Heal, W. P., Wright, M. H., Thinon, E. & Tate, E. W. Multifunctional protein labeling via enzymatic  
363 N-terminal tagging and elaboration by click chemistry. *Nat Protoc* **7**, 105-117 (2011).  
364 <https://doi.org/10.1038/nprot.2011.425>
- 365 15 Ibrahim, L., Stanton, C., Nutsch, K., Nguyen, T., Li-Ma, C., Ko, Y., Lander, G. C., Wiseman, R. L.,  
366 & Bollong, M. J. Succinylation of a KEAP1 sensor lysine promotes NRF2 activation. *Cell Chem*  
367 *Biol* **30**, 1295-1302.e1294 (2023). <https://doi.org/10.1016/j.chembiol.2023.07.014>
- 368 16 Umezawa, K., Tsumoto, H., Kawakami, K. & Miura, Y. A chemical probe for proteomic analysis  
369 and visualization of intracellular localization of lysine-succinylated proteins. *Analyst* **148**, 95-104  
370 (2022). <https://doi.org/10.1039/d2an01370c>
- 371 17 Afonso, C. F., Marques, M. C., António, J. P. M., Cordeiro, C., Gois, P. M. P., Cal, P. M. S. D., &  
372 Bernardes, G. J. L. Cysteine-Assisted Click-Chemistry for Proximity-Driven, Site-Specific  
373 Acetylation of Histones. *Angew Chem Int Ed Engl* **61**, e202208543 (2022).  
374 <https://doi.org/10.1002/anie.202208543>
- 375 18 Yang, Y. Y., Ascano, J. M. & Hang, H. C. Bioorthogonal chemical reporters for monitoring protein  
376 acetylation. *J Am Chem Soc* **132**, 3640-3641 (2010). <https://doi.org/10.1021/ja908871t>
- 377 19 Zhang, X. & Zhang, Y. Applications of azide-based bioorthogonal click chemistry in glycobiology.  
378 *Molecules* **18**, 7145-7159 (2013). <https://doi.org/10.3390/molecules18067145>
- 379 20 Jiang, H., Zheng T, Lopez-Aguilar A, Feng L, Kopp F, Marlow FL, Wu P. Monitoring dynamic  
380 glycosylation in vivo using supersensitive click chemistry. *Bioconjug Chem* **25**, 698-706 (2014).  
381 <https://doi.org/10.1021/bc400502d>
- 382 21 Bao, X., Zhao, Q., Yang, T., Fung, Y. M. & Li, X. D. A chemical probe for lysine malonylation.  
383 *Angew Chem Int Ed Engl* **52**, 4883-4886 (2013). <https://doi.org/10.1002/anie.201300252>
- 384 22 Zhang, Z., Tan, M., Xie, Z., Dai, L., Chen, Y., & Zhao, Y. Identification of lysine succinylation as  
385 a new post-translational modification. *Nature Chemical Biology* **7**, 58-63 (2011).  
386 <https://doi.org/10.1038/nchembio.495>

- 387 23 Wang, Z. A. & Cole, P. A. The Chemical Biology of Reversible Lysine Post-translational  
388 Modifications. *Cell Chem Biol* **27**, 953-969 (2020). <https://doi.org/10.1016/j.chembiol.2020.07.002>
- 389 24 Wang, Y., Chen, H. & Zha, X. Overview of SIRT5 as a potential therapeutic target: Structure,  
390 function and inhibitors. *Eur J Med Chem* **236**, 114363 (2022).  
391 <https://doi.org/10.1016/j.ejmech.2022.114363>
- 392 25 Zhu, S., Batushansky, A., Jopkiewicz, A., Makosa, D., Humphries, K. M., Van Remmen, H., &  
393 Griffin, T. M. Sirt5 Deficiency Causes Posttranslational Protein Malonylation and Dysregulated  
394 Cellular Metabolism in Chondrocytes Under Obesity Conditions. *Cartilage* **13**, 1185s-1199s  
395 (2021). <https://doi.org/10.1177/1947603521993209>
- 396 26 Liu, H., Rosol, T. J., Sathiaselan, R., Mann, S. N., Stout, M. B., & Zhu, S. Cellular carbon stress  
397 is a mediator of obesity-associated osteoarthritis development. *Osteoarthritis Cartilage* **29**, 1346-  
398 1350 (2021). <https://doi.org/10.1016/j.joca.2021.04.016>
- 399 27 Liu, H., Issa, D. D. & Zhu, S. SIRT5 DEFICIENCY CAUSES CHONDROCYTE METABOLIC  
400 DYSFUNCTION AND OSTEOARTHRITIS DURING AGING. *Osteoarthritis and Cartilage* **30**,  
401 S330-S331 (2022). <https://doi.org/10.1016/j.joca.2022.02.444>
- 402 28 Liu, H., Binoy A, Ren S, Martino TC, Miller AE, Willis CRG, Veerabhadraiah SR, Sukul A, Bons  
403 J, Rose JP, Schilling B, Jurynech MJ, Zhu S. Sirt5 regulates chondrocyte metabolism and  
404 osteoarthritis development through protein lysine malonylation. *bioRxiv* (2024).  
405 <https://doi.org/10.1101/2024.07.23.604872>
- 406 29 Galván-Peña, S., Carroll, R. G., Newman, C., Hinchy, E. C., Palsson-McDermott, E., Robinson, E.  
407 K., Covarrubias, S., Nadin, A., James, A. M., Haneklaus, M., Carpenter, S., Kelly, V. P., Murphy,  
408 M. P., Modis, L. K., & O'Neill, L. A. Malonylation of GAPDH is an inflammatory signal in  
409 macrophages. *Nat Commun* **10**, 338 (2019). <https://doi.org/10.1038/s41467-018-08187-6>
- 410 30 Xu, M., Tian, X., Ku, T., Wang, G. & Zhang, E. Global Identification and Systematic Analysis of  
411 Lysine Malonylation in Maize (*Zea mays* L.). *Front Plant Sci* **12**, 728338 (2021).  
412 <https://doi.org/10.3389/fpls.2021.728338>
- 413 31 Li, Z., Wu, Q., Zhang, Y., Zhou, X. & Peng, X. Systematic analysis of lysine malonylation in  
414 *Streptococcus mutans*. *Front Cell Infect Microbiol* **12**, 1078572 (2022).  
415 <https://doi.org/10.3389/fcimb.2022.1078572>
- 416 32 Nie, L. B., Liang, Q. L., Wang, M., Du, R., Zhang, M. Y., Elsheikha, H. M., & Zhu, X. Q. Global  
417 profiling of protein lysine malonylation in *Toxoplasma gondii* strains of different virulence and  
418 genetic backgrounds. *PLoS Negl Trop Dis* **16**, e0010431 (2022).  
419 <https://doi.org/10.1371/journal.pntd.0010431>

- 420 33 Du, Y., Cai, T., Li, T., Xue, P., Zhou, B., He, X., Wei, P., Liu, P., Yang, F., & Wei, T. . Lysine  
421 Malonylation Is Elevated in Type 2 Diabetic Mouse Models and Enriched in Metabolic Associated  
422 Proteins. *Molecular & Cellular Proteomics* **14**, 227-236 (2015).  
423 <https://doi.org/https://doi.org/10.1074/mcp.M114.041947>
- 424 34 Wu, L. F., Wang, D. P., Shen, J., Gao, L. J., Zhou, Y., Liu, Q. H., & Cao, J. M. Global profiling of  
425 protein lysine malonylation in mouse cardiac hypertrophy. *J Proteomics* **266**, 104667 (2022).  
426 <https://doi.org/10.1016/j.jprot.2022.104667>
- 427 35 Lu Zou, Y. Y. Z. W. X. F. X. H. J. S. T. L. H. M. T. Y. Lysine Malonylation and Its Links to  
428 Metabolism and Diseases. *Aging and disease* **14**, 84-98 (2023).
- 429 36 Rowland, L. A., Guilherme, A., Henriques, F., DiMarzio, C., Munroe, S., Wetoska, N., Kelly, M.,  
430 Reddig, K., Hendricks, G., Pan, M., Han, X., Ilkayeva, O. R., Newgard, C. B., & Czech, M. P. De  
431 novo lipogenesis fuels adipocyte autophagosome and lysosome membrane dynamics. *Nature*  
432 *Communications* **14**, 1362 (2023). <https://doi.org/10.1038/s41467-023-37016-8>
- 433